AIP | Applied Physics Letters

Influence of interfacial properties on thermal transport at gold:silicon contacts

J. C. Duda, C.-Y. P. Yang, B. M. Foley, R. Cheaito, D. L. Medlin et al.

Citation: Appl. Phys. Lett. **102**, 081902 (2013); doi: 10.1063/1.4793431
View online: http://dx.doi.org/10.1063/1.4793431
View Table of Contents: http://apl.aip.org/resource/1/APPLAB/v102/i8
Published by the American Institute of Physics.

Influence of interfacial properties on thermal transport at gold:silicon contacts

J. C. Duda,[1,a)] C.-Y. P. Yang,[2] B. M. Foley,[1] R. Cheaito,[1] D. L. Medlin,[2] R. E. Jones,[2] and P. E. Hopkins[1,b)]
[1]*Department of Mechanical and Aerospace Engineering, University of Virginia, Charlottesville, Virginia 22904, USA*
[2]*Sandia National Laboratories, Livermore, California 94550, USA*

(Received 24 December 2012; accepted 11 February 2013; published online 26 February 2013)

We measure the Kapitza conductances at Au:Si contacts from 100 to 296 K via time-domain thermoreflectance. Contacts are fabricated by evaporating Au films onto Si substrates. Prior to Au deposition, the Si substrates receive pretreatments in order to modify interfacial properties, i.e., bonding and structural disorder. Through the inclusion of a Ti adhesion layer and the removal of the native oxide, Kapitza conductance can be enhanced by a factor of four at 296 K. Furthermore, interfacial roughness is found to have a negligible effect, which we attribute to the already low conductances of poorly bonded Au:Si contacts. © *2013 American Institute of Physics*. [http://dx.doi.org/10.1063/1.4793431]

Solid-solid contacts will dictate the overall thermal performance of a given device when its characteristic lengths approach the mean-free-paths of the pertinent thermal carriers due to the fact that these interfaces provide additional sites for carrier scattering.[1,2] In semiconductor technologies, thermal transport is often mediated by phonons. While many early attempts to quantify the phonon mean-free-path relied heavily on the gray approximation (where a single value is assumed regardless of phonon frequency or wavevector), it has recently become commonplace to consider the entire spectrum of mean-free-paths in a given material.[3–5] For example, it has been shown that the mean-free-paths of phonons contributing to thermal transport in Si can span from a few Ångströms to upwards of several microns.[6,7] This range of scales overlaps with that of the architectures typical of Si-based nanostructures and devices, thereby indicating that interfaces can be a primary source of thermal resistance in such systems.

While Au:Si contacts remain ubiquitous in modern electronics, thermal characterization remains limited. Tas *et al.*[8] employed picosecond acoustics to study the influence of interfacial bonding at Au:Si contacts via ion implantation, effectively identifying how interface non-idealities, e.g., the presence of impurities or weak bonding, can affect low frequency phonon transmission. In that work, they found that ion implantation led to higher transmission coefficients, which they attributed to interfacial stiffening. Stevens *et al.*[9] measured the room temperature Kapitza conductance at an interface between a thin Au film and Si substrate to be 71 MW m^{-2} K^{-1} via pump-probe optical thermometry, although no details about interfacial properties were provided. However, this missing information is critical, as interfacial structure[10–15] and bonding[16–21] can have a marked effect on thermal transport. For example, Oh *et al.*[22] measured the thermal conductance at junctions between transfer-printed and sputtered Au films and hydrogen-terminated Si where conductances were 43 and 119 MW m^{-2} K^{-1} at room temperature, respectively. This threefold difference in conductance between the two interfaces comprised of the same materials illustrates how dramatically interfacial properties can affect thermal transport.

In this letter, we report low-frequency coherent phonon transmissivities, $\mathscr{T}$, and Kapitza conductances, h_K, at Au:Si contacts from 100 to 296 K as measured via time-domain thermoreflectance (TDTR). A series of Au:Si contacts were fabricated by evaporating thin Au films onto Si substrates. Prior to Au deposition, the Si substrates received pretreatments in order to modify interfacial properties, i.e., structure and bonding. Changes in structure were achieved through etching to control both interfacial roughness and the presence of an oxide layer, while changes in bonding were achieved through the inclusion of a Ti adhesion layer. The influence of interfacial roughness was found to have a significant effect on low-frequency (≈80 GHz) coherent phonon transmission, but a much smaller and non-monotonic effect on Kapitza conductance. The addition of a Ti adhesion layer and the removal of the native oxide layer separately resulted in nearly twofold increases in Kapitza conductance at 296 K. The data indicate that poor adhesion between film and substrate (absence of a Ti adhesion layer) or structural and compositional disorder (presence of a native α:SiO_2 layer) drastically reduce the temperature dependence of Kapitza conductance, indicating that interfacial non-idealities impede anharmonic phonon-phonon interactions that would otherwise contribute to interfacial thermal transport. Finally, these data suggest that the properties of the interface can have an equivalent, if not greater, influence on Kapitza conductance than the inherent vibrational mismatch between the materials comprising the interface.

To begin, prime-grade, boron-doped ⟨100⟩ silicon wafers were cleaved and sequentially cleaned with methanol, acetone, isopropanol, and deionized water. Between each successive clean, the samples were dried with nitrogen. After cleaning, samples were treated with a 5:1 buffered oxide etch (BOE) for 30 s to remove the native oxide, rinsed in deionized water, and dried again with nitrogen. Several samples (B, C,

a)Electronic mail: duda@virginia.edu.
b)Electronic mail: phopkins@virginia.edu.

TABLE I. Sample details for Au:Si contacts.

	Sample	Etch time (s)	δ_{rms} (nm)	d_{Au} (nm)	d_{SiO_2} (nm)	d_{Ti} (nm)
$\mathscr{T}$ Series	A	0	<0.10	20 ± 2	2	0
	B	30	3.16	20 ± 2	2	0
	C	90	1.00	20 ± 2	2	0
	D	180	28.6	20 ± 2	2	0
h_K Series	E	0	0.52	80 ± 5	2	0
	F	30	2.82	80 ± 5	2	0
	G	90	1.38	80 ± 5	2	0
	H	180	21.2	80 ± 5	2	0
	I	0	0.64	80 ± 5	2	7 ± 3
	J	0	0.58	80 ± 5	<0.1	7 ± 3

D, F, G, H) were then submersed in tetramethyl ammonium hydroxide solution heated to 80 °C for the times listed in Table I. Note that the etch times and roughnesses do not necessarily correlate, as different strength solutions were used to induce varying degrees of roughness. Native oxide layers were then allowed to reform through exposure to ambient for 48 h. Atomic force microscopy (AFM) was used to measure the root-mean-square (rms) roughness of each sample. Before film deposition, sample J was once again treated with BOE to remove the native oxide. Gold (and Ti for samples I and J) films of varying thickness were then e-beam evaporated using planetary rotation.

We also conducted cross-sectional transmission electron microscopy to investigate the interfacial configurations. Specimens were prepared by focused ion beam (FIB) thinning and were examined using an FEI Titan™ G2 80-200 scanning transmission electron microscope (STEM) equipped with a SuperX™ 4-SDD windowless x-ray detector array and a high angle annular dark field (HAADF) detector. Figure 1 shows

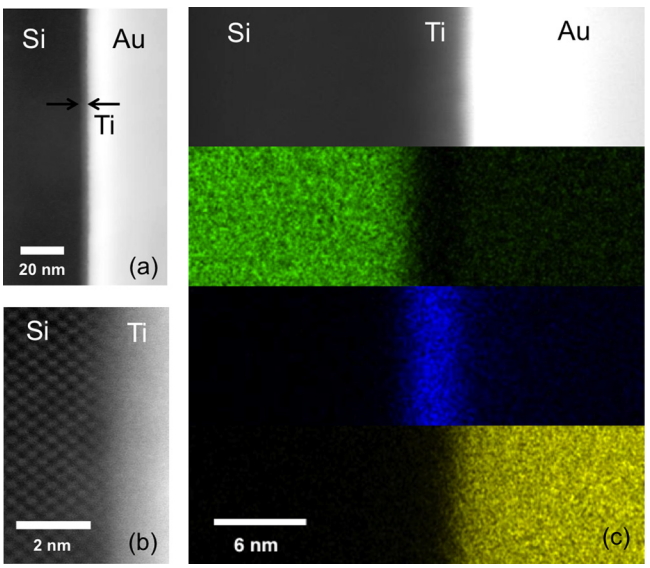

FIG. 1. STEM analysis of 80 nm Au on Si sample with native silicon oxide removed and Ti adhesion layer (sample J). (a) STEM (HAADF) image shows that Ti adhesion layer grows as a continuous and uniform deposit. (b) High resolution HAADF-STEM image shows that silicon remains crystalline up to the Ti layer. (c) EDS maps for Si (green), Ti (blue), and Au (yellow), show abruptly terminating compositional profiles indicating that the Ti layer prevents inter-reaction between the Au and Si.

results from sample J (native oxide removed, Ti adhesion layer). We also analyzed films prepared under equivalent conditions as those of samples E (native oxide present, no Ti adhesion layer) and I (native oxide present, with Ti adhesion layer). The results show that the Ti adhesion layer is a continuous and uniform deposit (Fig. 1(a)) and that the silicon is crystalline up to this layer (Fig. 1(b)). Energy dispersive x-ray spectroscopy (EDS) analysis (Fig. 1(c)) showed abruptly terminating compositional profiles indicating that the Ti interlayer prevented any significant interdiffusion or reaction between the gold and silicon. Equivalent results were observed for the samples analyzed with a native oxide present.

The low-frequency phonon transmissivities and Kapitza conductances at Au:Si interfaces were measured with TDTR.[23] In short, TDTR is a pump-probe optical thermometry technique; in our setup 100 fs laser pulses emanate from a Spectra Physics Tsunami at an 80 MHz repetition rate. We delay the time in which the probe pulse reaches the sample relative to the pump pulse by way of a mechanical delay stage. In this study, we frequency double the pump via a BiBO crystal to improve signal-to-noise through filtering while modulating the pump at 11.39 MHz. We monitor the ratio of the in-phase to out-of-phase signal of the probe beam from a lock-in amplifier ($-V_{in}/V_{out}$) as a function of probe delay time, t. Our pump and probe spots are focused to $1/e^2$ radii of 25 and 6 μm at the sample surface, respectively. We take a total of three TDTR measurements on each film. Phonon transmissivity measurements are made in ambient and Kapitza conductance measurements are made at temperatures from 100 to 296 K in a cryostat with optical access that is kept under vacuum.

Low-frequency phonon transmissivities at Au:Si interfaces (samples A through D, listed as $\mathscr{T}$ series in Table I) were determined as a function of interfacial roughness via picosecond acoustics. This technique relies on the subpicosecond nature of the pump heating event; the sudden heating of the film produces an oscillatory strain within the film that, in turn, produces an oscillatory component in the monitored thermoreflectance signal that persists for ≈60 ps.[8,24] The thicknesses of the Au films used for transmissivity measurements yield ≈80 GHz resonant frequencies.[25] The damping rate of the oscillatory signal can be used to determine phonon transmissivity by fitting the intensity of the thermoreflectance signal, I, with the expression,

$$I(t,T) = A\exp(-\Gamma t)\cos\left(\frac{2\pi}{T}t - \delta\right) - B\exp\left(-\frac{t}{\tau}\right), \quad (1)$$

and then relating the damping coefficient, Γ, and the period of oscillation, T, to transmissivity through the relationship,

$$1 - \mathscr{T} = \exp(-\Gamma T), \quad (2)$$

as is described in Ref. 24. An example of the raw intensity signal and the corresponding fit are shown in Fig. 2.

At longer probe delay times (300 ps < t < 5200 ps), we fit the TDTR data collected on samples E through J (listed at h_K series in Table I) with a thermal model that accounts for pulse accumulation in a layered system.[26–28] The temperature

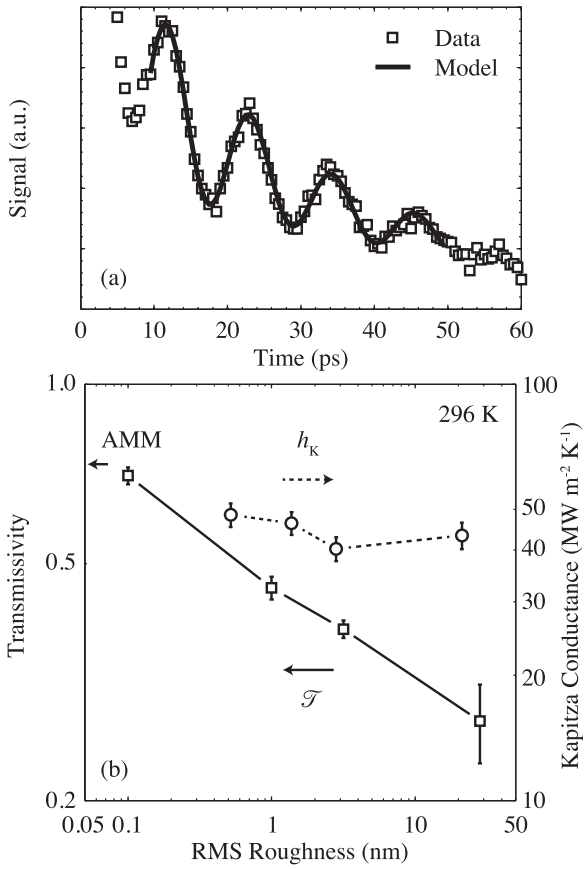

FIG. 2. (a) Example data depicting picosecond acoustic response from a 20 nm Au film on Si substrate. (b) Coherent phonon transmissivity and Kapitza conductance plotted as a function of interface RMS roughness. Error bars represent both the repeatability of the measurement as well as sensitivity to the variations in film thickness listed in Table I. While roughness affects both, the trends with roughness are dissimilar, indicating interfacial features affect ballistic and diffusive phonons differently.

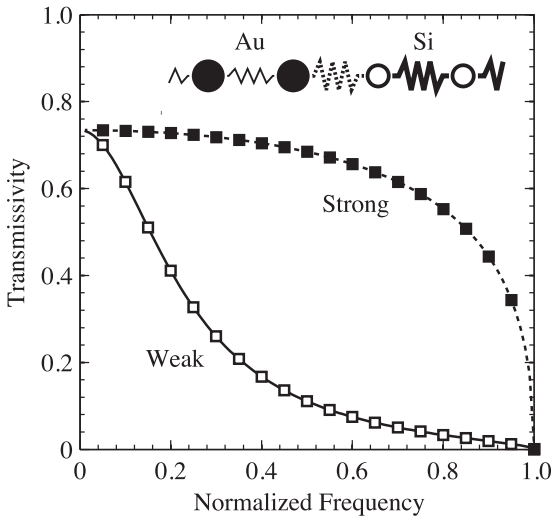

FIG. 3. Transmissivity a "Au:Si" contact as a function of normalized frequency as calculated via the non-equilibrium Green's function approach (see Ref. 37 for details). In the model, the ratio of acoustic impedances between the materials comprising the junction are equal to that between Au and Si. The weakly bonded system has an interfacial force constant 10% of the strongly bonded system. A weak interfacial bond impedes the transmission of high frequency phonons.

change at the surface is related to the thermal properties (thermal conductivity and heat capacity) of the individual layers, as well as the Kapitza conductance between layers. We assume bulk values for the thermal properties of the Au film and for the heat capacity of the Si substrate.[29] We then fit the data to a curve by adjusting the Kapitza conductance between at the Au:Si contact and the conductivity of the Si substrate.[30]

Room temperature phonon transmissivities and Kapitza conductances at Au:Si contacts are plotted as a function of interface roughness in Fig. 2(b). As is evident in the figure, low-frequency coherent phonon transmissivity is strongly dependent on interface roughness, and at nominally smooth interfaces, the measured transmissivity is nearly identical to that predicted by the acoustic mismatch model (AMM).[31] On the contrary, the effect of roughness on Kapitza conductance is less severe and non-monotonic, although the relative variation with roughness (≈20%) is consistent with earlier measurements of Kapitza conductance at rough Al:Si interfaces.[14] This is likely due to the fact that the poor adhesion between Au and α:SiO_2 (Ref. 32) readily impedes high-frequency vibrations from transmitting energy across the interface (see Fig. 3). In turn, roughness does not serve to further limit Kapitza conductance. Furthermore, the dissimilarities between the observed trends illustrate the differences between the coherent (ballistic) nature of the phonon transmissivity measurements as opposed to the incoherent (diffusive) nature of the Kapitza conductance measurements. In many ways, this is similar to the observed discrepancies between numerical studies implementing lattice-dynamical methods versus those employing molecular dynamics simulations;[33–35] that is, properties of the interface affect ballistic and diffusive phonons differently. Furthermore, this distinction between diffusive and ballistic phonon transport has been a centerpiece of many reports on the thermal behavior of superlattices.[36]

The Kapitza conductances at several of our Au:Si contacts are plotted as a function of temperature in Fig. 4. We also plot the measured conductances at interfaces between both sputtered and transfer-printed Au films and hydrogen-terminated Si from Ref. 22. In addition, the predictions of the diffuse mismatch model (DMM)[38,39] and the maximum transmission model (MTM)[40] are plotted for comparison. The temperature dependencies of these models are indicative of the assumed phonon-phonon interactions. That is, the DMM assumes elastic phonon-phonon interactions and thus begins to level off above the Debye temperature of Au, $\theta_{Au} = 165$ K. On the other hand, the MTM also allows for inelastic (anharmonic) phonon-phonon interactions and thus predicts an increase in conductance with increasing temperature above 165 K.

As is evident in the plot, both the presence of the native oxide layer or the absence of a Ti adhesion layer lead not only to lower Kapitza conductances, but also a significantly diminished temperature dependence. This data indicates that interfacial non-idealities, i.e., weak bonding between Au and α:SiO_2 or structural disorder due to an amorphous interfacial oxide, impede anharmonic phonon-phonon interactions that would otherwise contribute to interfacial thermal transport. This result is consistent with earlier experimental[14,21] and computational[15,19] studies. However, unique to this data set is the fact that the room temperature Kapitza conductance at

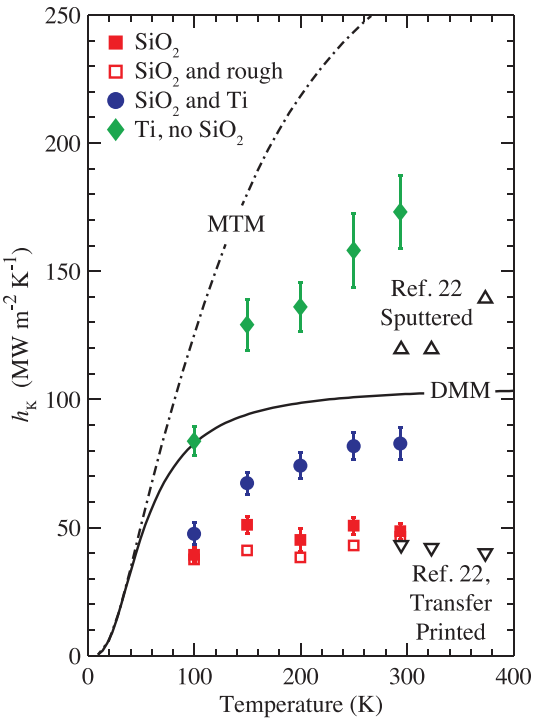

FIG. 4. Kapitza conductance at Au:Si contacts plotted as a function of temperature. Error bars represent both the repeatability of the measurement as well as sensitivity to the variations in film thickness listed in Table I. The predictions of the DMM and the MTM are plotted as the solid and dash-dot lines, respectively. Kapitza conductance at a roughened Au:Si contact (hollow squares, sample G) closely follows that of the nominally flat contact (filled squares, sample E). The inclusion of a Ti adhesion layer (circles, sample I) increases conductance by 70% at room temperature, while the inclusion of Ti combined with the removal of the native oxide (diamonds, sample J) increases conductance by more than a factor of 3. Upward and downward triangles are conductance data taken at interfaces between Au films and hydrogen-terminated Si from Ref. 22.

these interfaces span from 46 to 173 $\mathrm{MW\,m^{-2}\,K^{-1}}$, as opposed to the factor of 2 to 3 seen in earlier works. Whereas the efficiency of thermal transport at interfaces is often thought to be a manifestation of the relative match or mismatch between the vibrational properties of the constituent materials, these data suggest that the properties of the interface can have as much, if not more, influence. For example, compare the Kapitza conductance at a Au:Si contact (with oxide, 46 $\mathrm{MW\,m^{-2}\,K^{-1}}$) to a previously reported measurement of Kapitza conductance at an Al:Si from Ref. 41 (also with oxide, 172 $\mathrm{MW\,m^{-2}\,K^{-1}}$). This factor of four difference in Kapitza conductance is due to the unique vibrational spectra of Au and Al, where the maximum phonon frequencies differ by a factor of two. However, in a single material system, e.g., Au:Si, we also observe a factor of four difference in Kapitza conductance due only to the modification of the interface.

In summary, we have measured the Kapitza conductances at Au:Si contacts from 100 to 296 K via time-domain thermoreflectance. The interfacial properties of these contacts were modified through via etching and through the inclusion of a Ti adhesion layer, thus providing a means to vary interfacial bonding and structural disorder. Through the inclusion of a Ti adhesion layer and the removal of the native oxide, it was shown that Kapitza conductance at Au:Si contacts can be enhanced by a factor of four at 296 K. Furthermore, interfacial roughness is found to have a negligible effect, which has been attributed to the already low conductances of poorly bonded Au:Si contacts.

J.C.D. and P.E.H. acknowledge funding from the National Science Foundation (CBET-1134311). J.C.D. would like to thank M.S.M. for insightful discussions. This work was supported in part by the Laboratory Directed Research and Development (LDRD) program at Sandia National Laboratories. Sandia is a multi-program laboratory managed and operated by Sandia Corporation, a wholly owned subsidiary of Lockheed Martin Corporation, for the U.S. Department of Energy's National Nuclear Security Administration under contract DE-AC04-94AL85000.

[1]D. G. Cahill, W. K. Ford, K. E. Goodson, G. D. Mahan, A. Majumdar, H. J. Maris, R. Merlin, and S. R. Phillpot, J. Appl. Phys. **93**, 793 (2003).
[2]G. Chen, *Nanoscale Energy Transport and Conversion: A Parallel Treatment of Electrons, Molecules, Phonons, and Photons* (Oxford University Press, New York, New York, 2005).
[3]Z. Wang, J. E. Alaniz, W. Jang, J. E. Garay, and C. Dames, Nano Lett. **11**, 2206 (2011).
[4]R. Cheaito, J. C. Duda, T. E. Beechem, K. Hattar, J. F. Ihlefeld, D. L. Medlin, M. A. Rodriguez, M. J. Campion, E. S. Piekos, and P. E. Hopkins, Phys. Rev. Lett. **109**, 195901 (2012).
[5]B. M. Foley, H. J. Brown-Shaklee, J. C. Duda, R. Cheaito, B. J. Gibbons, D. L. Medlin, J. F. Ihlefeld, and P. E. Hopkins, Appl. Phys. Lett. **101**, 231908 (2012).
[6]A. S. Henry and G. Chen, J. Comput. Theor. Nanosci. **5**, 141 (2008).
[7]D. P. Sellan, E. S. Landry, J. E. Turney, A. J. H. McGaughey, and C. H. Amon, Phys. Rev. B **81**, 214305 (2010).
[8]G. Tas, J. J. Loomis, H. J. Maris, A. A. Bailes III, and L. E. Seiberling, Appl. Phys. Lett. **72**, 2235 (1998).
[9]R. J. Stevens, A. N. Smith, and P. M. Norris, J. Heat Transfer **127**, 315 (2005).
[10]P. E. Hopkins, P. M. Norris, R. J. Stevens, T. E. Beechem, and S. Graham, J. Heat Transfer **130**, 062402 (2008).
[11]Y. Xu, R. Kato, and M. Goto, J. Appl. Phys. **108**, 104317 (2010).
[12]P. E. Hopkins, J. C. Duda, S. P. Clark, C. P. Hains, T. J. Rotter, L. M. Phinney, and G. Balakrishnan, Appl. Phys. Lett. **98**, 161913 (2011).
[13]G. Pernot, M. Stoffel, I. Savic, F. Pezzoli, P. Chen, G. Savelli, A. Jacquot, J. Schumann, U. Denker, I. Mönch, C. Deneke, O. G. Schmidt, J. M. Rampnoux, S. Wang, M. Plissonnier, A. Rastelli, S. Dilhaire, and N. Mingo, Nat. Mater. **9**, 491 (2010).
[14]J. C. Duda and P. E. Hopkins, Appl. Phys. Lett. **100**, 111602 (2012).
[15]J. C. Duda, T. S. English, E. S. Piekos, T. E. Beechem, T. W. Kenny, and P. E. Hopkins, J. Appl. Phys. **112**, 073519 (2012).
[16]M. Hu, P. Keblinski, and P. K. Schelling, Phys. Rev, B **79**, 104305 (2009).
[17]L. Hu, L. Zhang, M. Hu, J.-S. Wang, B. Li, and P. Keblinski, Phys. Rev. B **81**, 235427 (2010).
[18]K. C. Collins, S. Chen, and G. Chen, Appl. Phys. Lett. **97**, 083102 (2010).
[19]J. C. Duda, T. S. English, E. S. Piekos, W. A. Soffa, L. V. Zhigilei, and P. E. Hopkins, Phys. Rev. B **84**, 193301 (2011).
[20]M. Shen, W. J. Evans, D. Cahill, and P. Keblinski, Phys. Rev. B **84**, 195432 (2011).
[21]P. E. Hopkins, M. Baraket, E. V. Barnat, T. E. Beechem, S. P. Kearney, J. C. Duda, J. T. Robinson, and S. G. Walton, Nano Lett. **12**, 590 (2012).
[22]D.-W. Oh, S. Kim, J. A. Rogers, D. G. Cahill, and S. Sinha, Adv. Mater. **23**, 5028 (2011).
[23]D. G. Cahill, K. Goodson, and A. Majumdar, J. Heat Transfer **124**, 223 (2002).
[24]M. D. Losego, M. E. Grady, N. R. Sottos, D. G. Cahill, and P. V. Braun, Nat. Mater. **11**, 502 (2012).
[25]C. Thomsen, J. Strait, Z. Vardeny, H. J. Maris, J. Tauc, and J. J. Hauser, Phys. Rev. Lett. **53**, 989 (1984).
[26]D. G. Cahill, Rev. Sci. Instrum. **75**, 5119 (2004).
[27]A. J. Schmidt, X. Chen, and G. Chen, Rev. Sci. Instrum. **79**, 114902 (2008).
[28]P. E. Hopkins, J. R. Serrano, L. M. Phinney, S. P. Kearney, T. W. Grasser, and C. T. Harris, J. Heat Transfer **132**, 081302 (2010).
[29]C. Y. Ho, R. W. Powell, and P. E. Liley, J. Phys. Chem. Ref. Data **1**, 279 (1972).

[30]R. J. Stoner and H. J. Maris, Phys. Rev. B **48**, 16373 (1993).
[31]W. A. Little, Can. J. Phys. **37**, 334 (1959).
[32]H. Dallaporta and A. Cros, Appl. Phys. Lett. **48**, 1357 (1986).
[33]W. Zhang, T. S. Fisher, and N. Mingo, J. Heat Transfer **129**, 483 (2007).
[34]E. S. Landry and A. J. H. McGaughey, Phys. Rev. B **80**, 165304 (2009).
[35]E. S. Landry and A. J. H. McGaughey, J. Appl. Phys. **107**, 013521 (2010).
[36]Y. K. Koh, Y. Cao, D. G. Cahill, and D. Jena, Adv. Funct. Mater. **19**, 610 (2009).
[37]P. E. Hopkins, P. M. Norris, M. S. Tsegaye, and A. W. Ghosh, J. Appl. Phys. **106**, 063503 (2009).
[38]E. T. Swartz and R. O. Pohl, Rev. Mod. Phys. **61**, 605 (1989).
[39]J. C. Duda, T. E. Beechem, J. L. Smoyer, P. M. Norris, and P. E. Hopkins, J. Appl. Phys. **108**, 073515 (2010).
[40]C. Dames and G. Chen, J. Appl. Phys. **95**, 682 (2004).
[41]P. E. Hopkins, J. C. Duda, C. W. Petz, and J. A. Floro, Phys. Rev. B **84**, 035438 (2011).